

## Effect of boron/phosphorus-containing additives on electrodeposited CoNiFe soft magnetic thin films

Jian-mei LI<sup>1</sup>, Zhao ZHANG<sup>2</sup>, Jin-feng LI<sup>3</sup>, Min-zhao XUE<sup>1</sup>, Yan-gang LIU<sup>1</sup>

1. School of Chemistry and Chemical Technology, Shanghai Jiao Tong University, Shanghai 200240, China;

2. Department of Chemistry, Zhejiang University, Hangzhou 310027, China;

3. School of Materials Science and Engineering, Central South University, Changsha 410083, China

Received 21 October 2011; accepted 17 December 2012

**Abstract:** CoNiFe, CoNiFeB and CoNiFeP soft magnetic thin films were prepared by cyclic voltammetry method. The morphologies, composition and structures were characterized by scanning electron microscope (SEM), energy-dispersive X-ray spectroscopy (EDS) and X-ray diffractometer (XRD). The soft magnetic properties were investigated through vibrating sample magnetometer (VSM). The corrosion resistance was investigated through Tafel polarization and electrochemical impedance spectroscopic (EIS). The results show that all the electrodeposited CoNiFe, CoNiFeB and CoNiFeP films are mixtures of crystalline and amorphous phases, and high amount of boron/phosphorus-containing additives favors the formation of amorphous state. Nanostructure is obtained in CoNiFe and CoNiFeB films. The inclusion of boron causes the film more dense and also increases its corrosion resistance. Meanwhile, the inclusion of boron lowers its coercivity ( $H_c$ ) from 851.48 A/m to 604.79 A/m, but the saturation magnetic flux density ( $B_s$ ) is almost unchanged. However, the addition of phosphorus greatly increases the film particle size and decreases its corrosion stability. The coercivity ( $H_c$ ) of CoNiFeP film is also highly increased to 12485.79 A/m, and its saturation magnetic flux density ( $B_s$ ) is greatly decreased to 1.25 T.

**Key words:** magnetic materials; thin films; electrodeposition; magnetic properties; corrosion

### 1 Introduction

Magnetic materials are classified as soft if they have a low coercivity (the critical field strength  $H_c$  required to flip the direction of magnetization) [1]. Soft magnetic materials are central components of electromagnetic devices, and miniaturization of these devices requires materials with a very high saturation magnetic flux density ( $B_s$ ) [1]. Furthermore, high corrosion resistance is desired to improve the reliability of the devices [2].

Recently, materials other than plated permalloy such as CoNiFe, CoNiFeS, CoFe, CoFeSnP, CoFeCu, CoFeB and CoFeP have been investigated [3–5]. A strong candidate for replacement of NiFe in many micro-electro mechanical system (MEMS) applications is ternary CoNiFe alloy due to its possibility of achieving a high saturation magnetic flux density  $B_s$  combined with reasonably low  $H_c$  [6]. However, the physicochemical properties of CoNiFe alloy are greatly affected by their

compositions and microstructures [2,7]. Now, a lot of efforts have been done to prepare alloys with nanostructures through electrodeposition because nanostructured alloys are expected to possess good physicochemical properties, such as high hardness, good anti-fatigue characteristics and high saturation magnetic properties [8,9].

Electrodeposition represents a simple, cost-effective way of fabricating magnetic thin films, and it is suitable for integration of magnetic materials into MEMS devices [10]. The cyclic voltammetry (CV) is one of the most promising electrochemical techniques due to its ability to control grain size of the deposit [6,11]. The effects of organic and inorganic additives such as thiourea, sodium lauryl sulfate, DPS and saccharin on current efficiency, alloy composition, magnetic properties, morphology and stresses in the electrodeposited CoNiFe films have been thoroughly examined [4,10].

In our previous work [12,13], nanocrystalline CoNiFe thin films have been fabricated by cyclic

voltammetry technique, and its electrodeposition behavior has also been investigated using cyclic voltammetric and chronoamperometric experiments. In the present study, we try to prepare CoNiFeB/CoNiFeP thin films by the addition of boron/phosphorus-containing additives into the electrodeposition bath, and focus to investigate the influences of boron/phosphorus-containing additives on the structure, soft magnetic properties ( $H_c$ ,  $B_s$ ) and corrosion resistance of the electrodeposited films.

## 2 Experimental

The basic electrodeposition bath composition and additives are listed in Table 1. The film electrodeposited in  $\text{Na}_2\text{B}_4\text{O}_7$  additive-containing electrodeposition bath is designated for CoNiFeB thin film, and the film electrodeposited in  $\text{NaH}_2\text{PO}_2$  additive-containing electrodeposition bath for CoNiFeP thin film. Brass copper H63 ( $\text{Cu}_{64}\text{Zn}_{36}$ , hereinafter) rods embedded in Teflon with an exposure area of  $0.50\text{ cm}^2$  were used as the substrates. Before electroplating, the substrates were sequentially polished with 400# to 800# silicon carbide emery papers followed with  $2.5\text{ }\mu\text{m}$  alumina paste, rinsed with double distilled water, washed with acetone, rinsed with double distilled water again and then blow-dried by air. The thin films were electrodeposited on the brass copper rod using cyclic voltammetry (CV) in the potential range of  $-0.39\text{--}-1.19\text{ V}$  with a scanning rate of  $20\text{ mV/s}$ . It was operated in a three-electrode cell at room temperature ( $25\text{ }^\circ\text{C}$ ). The brass copper H63 rod was used as working electrode, a large platinum foil as counter electrode, and a saturated calomel electrode (SCE) as reference electrode, respectively. A salt bridge was used to minimize errors due to IR drop in the electrolytes. All potentials were referred to SCE. Mechanical impeller agitation with a rotating speed of  $1000\text{ r/min}$  was applied during the electrodeposition. For

the electrodeposition of each thin film, 6 CV cycles were performed. After the electrodeposition, the samples were rinsed with double distilled water and then dried in the air, and finally kept in a vacuum box at room temperature before analysis.

The electrodeposited film morphology was observed using SEM (Hitachi S-4700). Its composition was analyzed through EDS. The phase components and crystal structure were analyzed using XRD (D/max-2550 PC). A vibrating sample magnetometer (VSM) (Lakeshore 7407) was used to investigate their magnetic hysteresis loops, the coercivity and saturation magnetic flux density were obtained from the magnetic hysteresis loops.

Corrosion resistance is considered an indication of durability of the film material [14]. The corrosion behaviors of the electrodeposited CoNiFe, CoNiFeB and CoNiFeP soft magnetic thin films were investigated in the stationary neutral 3.5% NaCl solution by using Tafel polarization and EIS tests in a three-electrode cell as above. Here, the working electrode is the brass copper H63 covered with the electrodeposited film. After the measurement of open circuit potential (OCP), Tafel polarization was conducted with a commercial electrochemical workstation (CHI660A, China) and always initiated from OCP of  $0.25\text{ V}$  with a scanning rate of  $1\text{ mV/s}$  in a positive direction. EIS measurement was performed using a potentiostat coupled with a lock-in amplifier (IM6e, Australia) at OCP and carried out in the frequency ranging from  $100\text{ kHz}$  to  $0.01\text{ Hz}$ . The applied sinusoid signal amplitude was  $5\text{ mV}$ .

## 3 Results and discussion

### 3.1 Morphology, composition and structure of deposits

For the electrodeposited films, the thickness is  $2.5\text{--}3.0\text{ }\mu\text{m}$ . The effects of additives of  $\text{Na}_2\text{B}_4\text{O}_7$  and  $\text{NaH}_2\text{PO}_2$  on the surface morphologies are evident in the representative SEM images displayed in Figs. 1–3. Figure 1 shows the SEM images of the CoNiFe film electrodeposited in the bath without  $\text{Na}_2\text{B}_4\text{O}_7$  and  $\text{NaH}_2\text{PO}_2$  additives. The grain size is very fine and uniform. From Fig. 1(b), it can be seen that the grain size is less than  $50\text{ nm}$ . Some very small pores are also observed. EDS analysis indicates that the CoNiFe film consists of 58% Co, 13% Ni and 29% Fe.

For the CoNiFeB film electrodeposited in the bath containing additive of  $\text{Na}_2\text{B}_4\text{O}_7\cdot 10\text{H}_2\text{O}$ , the morphology (Fig. 2) is very similar to those of CoNiFe in Fig. 1, spherical and uniform nanoparticles are clearly observed, indicating that additives containing B have little effect on

**Table 1** Basic bath composition and additives for electrodeposition

Electrolyte composition	Additive	Electrodeposition conditions
13.9 g/L $\text{FeSO}_4\cdot 7\text{H}_2\text{O}$ , 33.7 g/L $\text{CoSO}_4\cdot 7\text{H}_2\text{O}$ , 21.0 g/L $\text{NiSO}_4\cdot 6\text{H}_2\text{O}$ , 14.2 g/L $\text{Na}_2\text{SO}_4$ , 41.2 g/L $\text{NH}_4\text{Cl}$ , 24.7 g/L $\text{H}_3\text{BO}_3$	0–40 g/L $\text{Na}_2\text{B}_4\text{O}_7\cdot 10\text{H}_2\text{O}$ or 0–40 g/L $\text{NaH}_2\text{PO}_2\cdot \text{H}_2\text{O}$	Bath pH 2.0  Bath temperature $40\text{ }^\circ\text{C}$  CV potential range $-0.39\text{--}-1.19\text{ V}$  CV Scanning rate $20\text{ mV/s}$

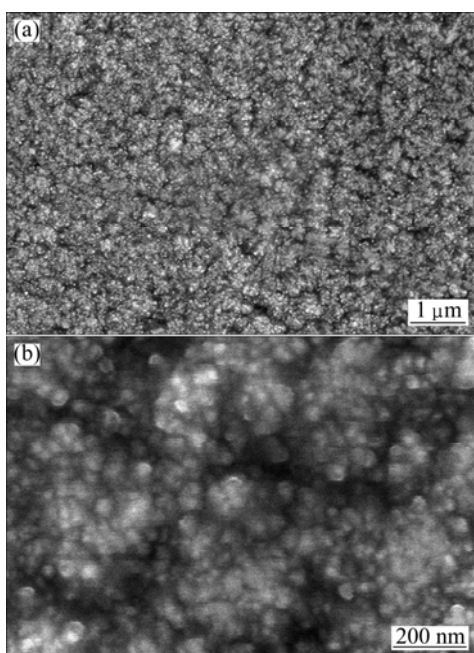


**Fig. 1** SEM images of electrodeposited CoNiFe film

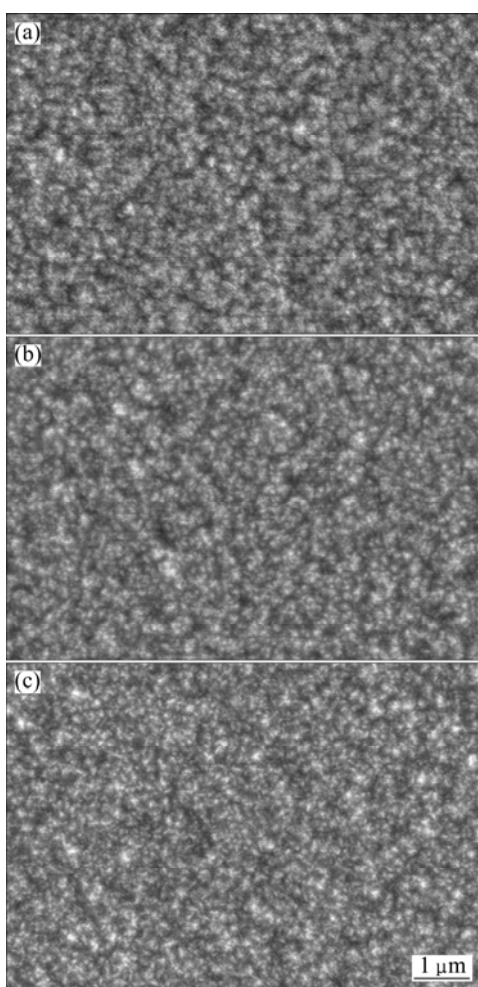


**Fig. 2** SEM images of CoNiFeB film electrodeposited in bath containing  $\text{Na}_2\text{B}_4\text{O}_7 \cdot 10\text{H}_2\text{O}$  additive of 4 g/L (a), 20 g/L (b) and 40 g/L (c)

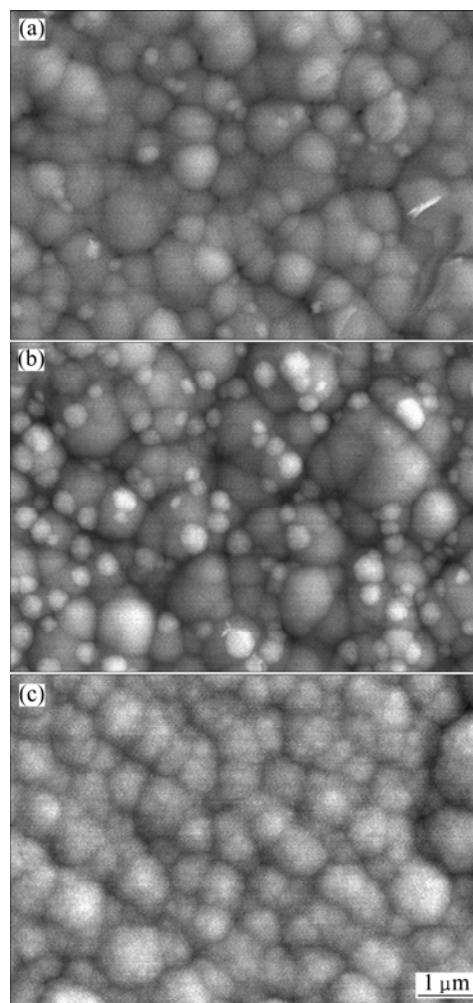


**Fig. 3** SEM images of CoNiFeP film electrodeposited in bath containing  $\text{NaH}_2\text{PO}_2 \cdot \text{H}_2\text{O}$  additive of 4 g/L (a), 16 g/L (b) and 40 g/L (c)

the morphology (surface roughness) of the CoNiFe electrodeposited film. However, with increasing the  $\text{Na}_2\text{B}_4\text{O}_7 \cdot 10\text{H}_2\text{O}$  additive dosage from 0 to 40 g/L, it still can be found that the electrodeposited CoNiFeB film becomes much denser and the grain size becomes a little smaller. Although the electrodeposition bath contains much high content of boride-containing component (including buffered  $\text{H}_3\text{BO}_3$  of 24.7 g/L and  $\text{Na}_2\text{B}_4\text{O}_7 \cdot 10\text{H}_2\text{O}$  changing from 4 to 40 g/L), the content of B element in the electrodeposited CoNiFeB film cannot be clearly detected through EDS. This is due to the fact that the mole fraction of B is too low to be detected. Because the boron content in the film was not detected using other methods such as secondary ion mass spectroscopy, it is temporarily unable to determine the content of B in the electrodeposited film. However, from the XRD patterns and corrosion behaviors described later, it can be confirmed that B element should exist in the film.

For the CoNiFeP film electrodeposited in the bath

containing additive of  $\text{NaH}_2\text{PO}_2 \cdot \text{H}_2\text{O}$ , the surface morphology changes dramatically. Compared with the CoNiFe film electrodeposited in the bath without  $\text{NaH}_2\text{PO}_2$  additive, its particle size is greatly increased to about  $1 \mu\text{m}$  (Fig. 3). Meanwhile, EDS analysis reveals that when  $4 \text{ g/L}$   $\text{NaH}_2\text{PO}_2 \cdot \text{H}_2\text{O}$  is added, the electrodeposited film contains  $6.02\%$  phosphorus. As the additive is increased to  $40 \text{ g/L}$ , the phosphorus content in film is increased a little to  $7.04\%$ .

The XRD patterns of the CoNiFe, CoNiFeB and CoNiFeP films electrodeposited in the additive-free bath and in the bath containing the additives of  $\text{Na}_2\text{B}_4\text{O}_7$  or  $\text{NaH}_2\text{PO}_2$  are shown in Figs. 4 and 5.  $\text{Co}_{0.7}\text{Fe}_{0.3}$  phase with BCC crystal structure is observed. In some samples, the electrode substrate of brass copper (CuZn alloy) is also detected by XRD, due to the thin thickness of the electrodeposited film. As the  $\text{Na}_2\text{B}_4\text{O}_7$  additive dosage in the electrodeposition bath increases, the diffraction peak is broadened a little, which reveals that the grain is refined a little. While, as the  $\text{NaH}_2\text{PO}_2$  additive dosage

increases, the diffraction peaks become weaker and weaker, which means that the crystal amount decreases, amorphous state is formed and its amount increases. Therefore, the electrodeposited film is a mixture of crystalline and/or amorphous phases. Especially, for the CoNiFeP film, as the  $\text{NaH}_2\text{PO}_2 \cdot \text{H}_2\text{O}$  additive dosage is increased to  $40 \text{ g/L}$ , complete amorphous state is confirmed by the broad diffusion halo (curve (d) in Fig. 5).

Interestingly, no diffraction peaks in Figs. 4 and 5 corresponding to boron, phosphorus and even nickel can be detected. The included boron or phosphorus in the electrodeposited CoNiFeB or CoNiFeP films should exist in an amorphous state, which may be deduced from the elevation of the XRD lines in the low diffraction angle region ( $2\theta$  less than  $50^\circ$ ). However, no diffraction peaks of nickel seem contradictory to the EDS analysis result. Generally, the peak of nickel crystal should be observed at  $2\theta$  of  $44.8^\circ$ ,  $52.2^\circ$  and  $76.7^\circ$  in the XRD pattern [15]. The reason may be attributed to the fact that the component nickel in the electrodeposited CoNiFe-base films exists in solid solutions as the amorphous state [8].

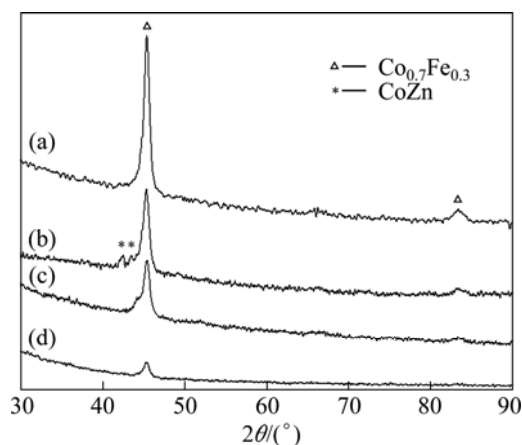


**Fig. 4** XRD patterns of CoNiFeB films electrodeposited in bath containing  $\text{Na}_2\text{B}_4\text{O}_7 \cdot 10\text{H}_2\text{O}$  additive with different dosages of  $0 \text{ g/L}$  (a),  $4 \text{ g/L}$  (b),  $20 \text{ g/L}$  (c) and  $40 \text{ g/L}$  (d)

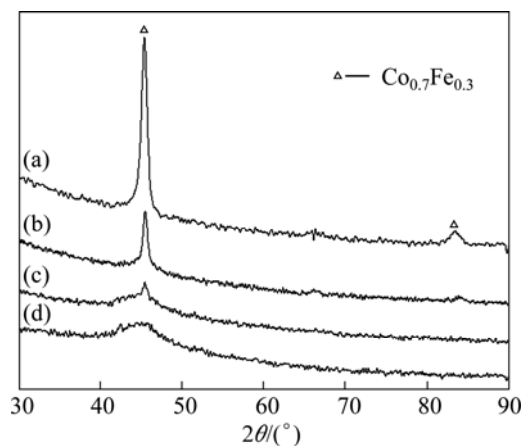


**Fig. 5** XRD patterns of CoNiFeP films electrodeposited in bath containing  $\text{NaH}_2\text{PO}_2 \cdot \text{H}_2\text{O}$  additive with different dosages of  $0 \text{ g/L}$  (a),  $4 \text{ g/L}$  (b),  $16 \text{ g/L}$  (c) and  $40 \text{ g/L}$  (d)

### 3.2 Magnetic properties of deposits

The plane magnetic hysteresis loops of the three films electrodeposited in the additive-free bath and in the bath with  $\text{Na}_2\text{B}_4\text{O}_7 \cdot 10\text{H}_2\text{O}$  additive of  $16 \text{ g/L}$  or  $\text{NaH}_2\text{PO}_2 \cdot \text{H}_2\text{O}$  additive of  $16 \text{ g/L}$  are illustrated in Fig. 6. The corresponding coercivity  $H_c$  and saturation magnetic flux density  $B_s$  are shown in Table 2. The CoNiFe film has a coercivity of  $851.48 \text{ A/m}$  and a saturation magnetic flux density of  $2.03 \text{ T}$ . For the CoNiFeB film electrodeposited in  $\text{Na}_2\text{B}_4\text{O}_7$  additive-containing bath, the coercivity is decreased to  $604.79 \text{ A/m}$ , while the saturation magnetic flux density is  $1.94 \text{ T}$ . Compared with CoNiFe film, there is almost no difference in saturation magnetic flux density. However, the electrodeposited CoNiFeP film exhibits a much higher coercivity of  $12485.79 \text{ A/m}$  and a much lower saturation magnetic flux density of  $1.25 \text{ T}$ , which means that the addition of  $\text{NaH}_2\text{PO}_2 \cdot \text{H}_2\text{O}$  to the electrodeposition bath sacrifices the magnetic properties of the electrodeposited films. It may result not only from the inclusion of impurity element P in the film, but also from the particle coarsening and structure variation.

**Table 2** Coercivity ( $H_c$ ) and saturation magnetization ( $B_s$ ) of three films electrodeposited in additive-free bath and in bath with  $16 \text{ g/L}$   $\text{Na}_2\text{B}_4\text{O}_7 \cdot 10\text{H}_2\text{O}$  or  $16 \text{ g/L}$   $\text{NaH}_2\text{PO}_2 \cdot \text{H}_2\text{O}$

Film	$B_s/\text{T}$	$H_c/(\text{A} \cdot \text{m}^{-1})$
CoNiFe	2.03	851.48
CoNiFeB	1.94	604.79
CoNiFeP	1.25	12485.79

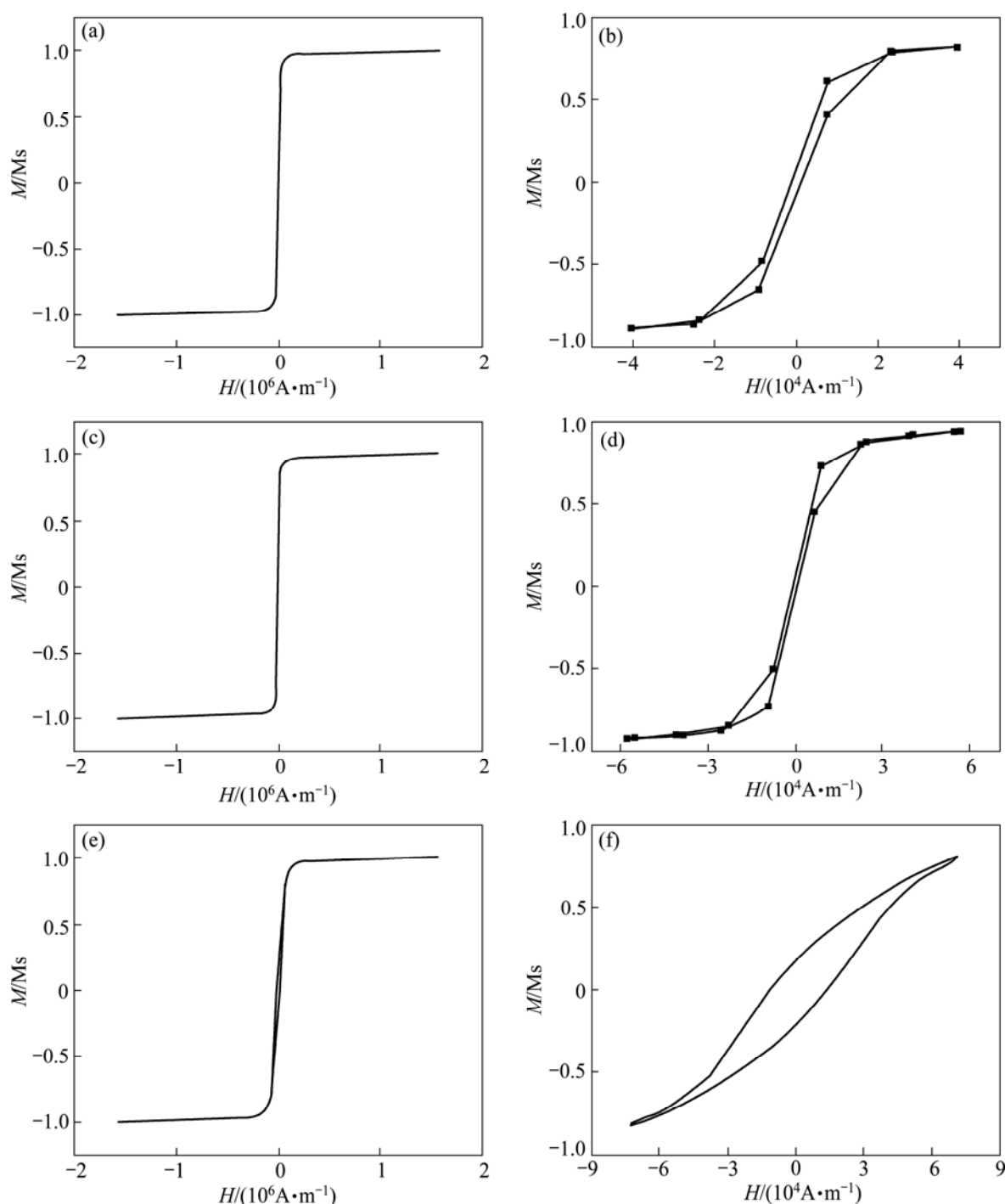


**Fig. 6** Plane hysteresis loops of CoNiFe films electrodeposited in baths without additives (a,b), with  $\text{Na}_2\text{B}_4\text{O}_7 \cdot 10\text{H}_2\text{O}$  additive (c,d) and with  $\text{NaH}_2\text{PO}_2 \cdot \text{H}_2\text{O}$  additive (e,f) ((a), (c), (e) Whole plane hysteresis loops; (b), (d), (f) Enlargement of central part)

In general, CoNiFe ternary alloy film exhibits good soft magnetic properties. However, the CoNiFe film electrodeposited in  $\text{Na}_2\text{B}_4\text{O}_7 \cdot 10\text{H}_2\text{O}$  containing bath possesses not only quite low coercivity of 604.79 A/m but also an acceptable saturation magnetic flux density of 1.94 T. The  $\text{Na}_2\text{B}_4\text{O}_7$  additive improves the soft magnetic properties of the electrodeposited film to some extent. While, P-containing additive deteriorates the soft magnetic properties.

### 3.3 Corrosion resistance of films

Tafel polarization curves and EIS plots of the CoNiFeB films electrodeposited in the bath containing different amount of  $\text{Na}_2\text{B}_4\text{O}_7$  additives are shown in Fig. 7. To compare the corrosion resistance difference, the Tafel polarization curve and EIS plot of CoNiFe film are also presented in Fig. 7. Figure 7(a) shows that the corrosion potential of CoNiFeB films (curves 2–4, ca. -300 mV) is much more positive than that of CoNiFe

film (curve 1, ca.  $-400$  mV). Meanwhile, the corrosion potential, which indicates the thermodynamic stability, moves positively with increasing  $\text{Na}_2\text{B}_4\text{O}_7 \cdot 10\text{H}_2\text{O}$  additive dosage in the electrodeposition bath. Figure 7(a) also shows that the corrosion current density is not greatly affected by the  $\text{Na}_2\text{B}_4\text{O}_7 \cdot 10\text{H}_2\text{O}$  dosage in the bath. Although B element cannot be detected through EDS, the electrochemical tests along with the microstructure observation and magnetic measurement indicate the existence of B element in the CoNiFeB film.

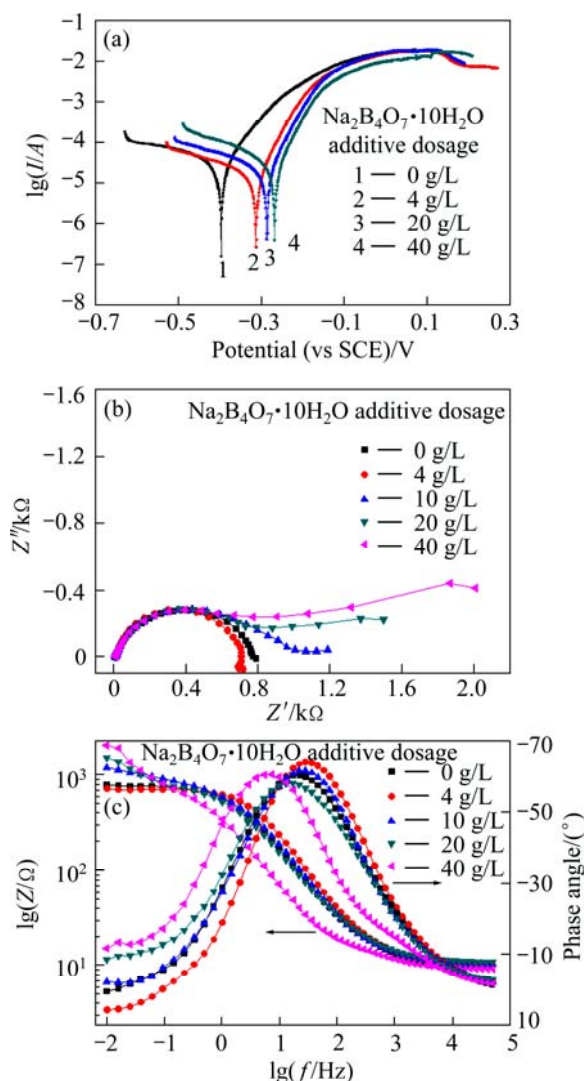


**Fig. 7** Tafel polarization curves (a), Nyquist (b) and Bode (c) plots of CoNiFeB film in 3.5% NaCl solution

The EIS plots of the CoNiFeB film consist of a high frequency capacitive loop and a low frequency loop. The high frequency parts of the Nyquist plots of CoNiFe and CoNiFeB films are almost overlapped (Fig. 7(b)), while the diameter of the low-frequency capacitive loop becomes larger with increasing the  $\text{Na}_2\text{B}_4\text{O}_7 \cdot 10\text{H}_2\text{O}$  additive dosage in the electrodeposited bath. It was proposed that the impedance at low frequencies (such as  $|Z|_{0.1 \text{ Hz}}$  or  $|Z|_{0.01 \text{ Hz}}$ ) could serve as an estimation of the

corrosion resistance [16,17]. Therefore, Fig. 7(c) clearly shows that the corrosion resistance of CoNiFeB films increases with the  $\text{Na}_2\text{B}_4\text{O}_7 \cdot 10\text{H}_2\text{O}$  additives in the electrodeposition bath.

Figure 8 shows the Tafel polarization curves and EIS plots of the CoNiFeP film electrodeposited in the bath containing different amount of  $\text{NaH}_2\text{PO}_2$  additive. The corrosion potential of the CoNiFeP films (curves 2–4, ca.  $-500$  mV) is more negative than that of the CoNiFe film (curve 1, ca.  $-400$  mV). Meanwhile, corresponding EIS results show that both the capacitive arc radii of the Nyquist plots (Fig. 8(b)) and  $|Z|_{0.1 \text{ Hz}}$  (Fig. 8(c)) decrease with the addition of  $\text{NaH}_2\text{PO}_2 \cdot \text{H}_2\text{O}$  to the electrodeposition bath. This indicates that the addition of  $\text{NaH}_2\text{PO}_2 \cdot \text{H}_2\text{O}$  to the electrodeposition bath deteriorates the corrosion resistance of CoNiFe films.

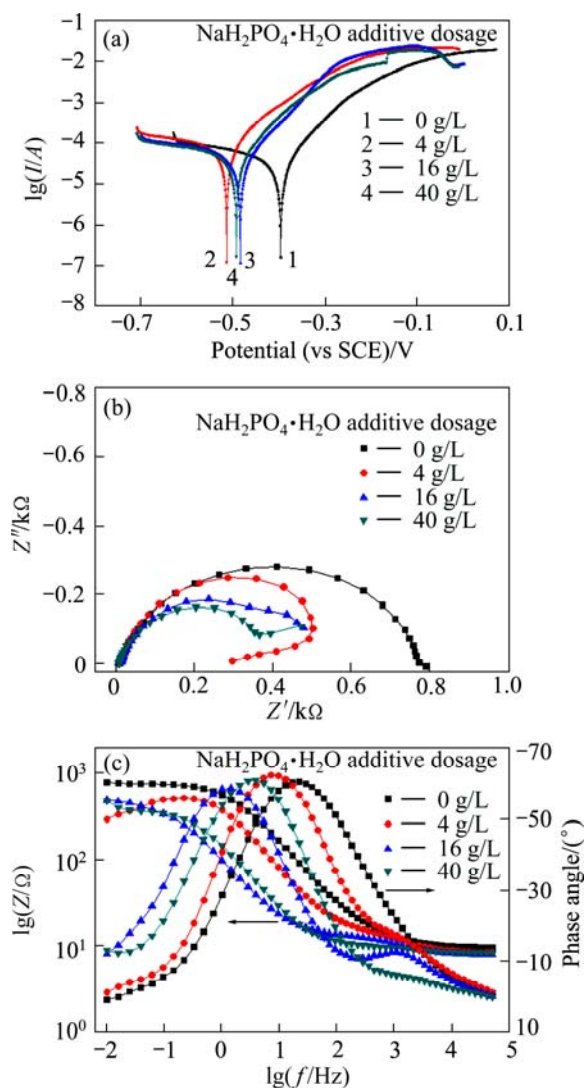


**Fig. 8** Tafel polarization curves (a) and Nyquist (b) and Bode (c) plots of CoNiFeP film in 3.5% NaCl solution

Therefore, compared with CoNiFe film, the boron-containing additive of  $\text{Na}_2\text{B}_4\text{O}_7$  increases the corrosion resistance, while the phosphorus-containing

additive of  $\text{NaH}_2\text{PO}_2$  lowers the corrosion resistance. It may result from the boron/phosphorus inclusion in the films and structure alteration.

## 4 Conclusions

1) All electrodeposited CoNiFe, CoNiFeB and CoNiFeP alloy films are mixtures of crystalline and amorphous phases; high content of boron/phosphorus-containing additives favors the formation of amorphous phase.

2) Nanostructure is obtained in CoNiFe and CoNiFeB film. Meanwhile, the inclusion of boron element causes the film more dense and increases the corrosion resistance.

3) The addition of phosphorus-containing additive greatly increases the film particle size and lowers its corrosion resistance.

4) CoNiFe film possesses a coercivity of 851.48 A/m and a saturation magnetic flux density of 2.03 T. The addition of boron lowers the coercivity to 604.79 A/m, and the saturation magnetic flux density is almost unchanged. While, the addition of phosphorus greatly deteriorates the soft magnetic properties with a coercivity of 12485.79 A/m and a saturation magnetic flux density of 1.25 T.

## References

- [1] OSAKA T, TAKAI M, HAYASHI K, OHASHI K, SAITO M, YAMADA K. A soft magnetic CoNiFe film with high saturation magnetic flux density and low coercivity [J]. *Nature*, 1998, 392(23): 796–798.
- [2] YOO B Y, HERNANDEZ S C, PARK D Y K, MYUNG N V. Electrodeposition of FeCoNi thin films for magnetic-MEMS devices [J]. *Electrochim Acta*, 2006, 51: 6346–6352.
- [3] TAKAI M, HAYASHI K, AOYAGI M, OSAKA T. Electrochemical preparation of soft magnetic CoNiFeS film with high saturation magnetic flux density and high resistivity [J]. *J Electrochem Soc*, 1997, 144(7): 203–204.
- [4] RHEN F M F, ROY S. Dependence of magnetic properties on micro-to nanostructure of CoNiFe films [J]. *J Appl Phys*, 2008, 103: 103901.
- [5] MISHRA A C, SAHOO T, SRINIVAS V, THAKUR A K. Giant magnetoimpedance in electrodeposited CoNiFe/Cu wire: A study on thickness dependence [J]. *Journal of Alloys and Compounds*, 2009, 480: 771–776.
- [6] RASMUSSEN F E, RAVNKILDE J T, TAN P T G, HANSEN O, BOUWSTRA S. Electroplating and characterization of cobalt–nickel–iron and nickel–iron for magnetic microsystems applications [J]. *Sensors and Actuators A*, 2001, 92: 242–248.
- [7] NAKANISHI T, OZAKI M, NAM H S, YOKOSHIMA T, OSAKA T. Pulsed electrodeposition of nanocrystalline CoNiFe soft magnetic thin films [J]. *J Electrochem Soc*, 2001, 148(9): C627–C631.
- [8] BAI A, HU C C. Iron-cobalt and iron-cobalt-nickel nanowires deposited by means of cyclic voltammetry and pulse-reverse electroplating [J]. *Electrochem Commun*, 2003, 5: 78–82.
- [9] ZHANG Y H, IVEY D G. Characterization of Co–Fe and Co–Fe–Ni soft magnetic films electrodeposited from citrate-stabilized sulfate baths [J]. *Materials Science and Engineering B*, 2007, 140: 15–22.
- [10] PARK D Y, YOO B Y, KELCHER S, MYUNG N V. Electrodeposition of low-stress high magnetic moment Fe-rich FeCoNi thin films [J]. *Electrochim Acta*, 2006, 51: 2523–2530.
- [11] ATALAY F E, KAYA H, ATALAY S. Effect of pH on the magnetoimpedance properties of electrodeposited CoNiFe microtubes [J]. *Physica B*, 2006, 371: 327–331.
- [12] CAI C, WANG Q P, ZHANG Z, YANG J F. Electrodeposition of nanocrystalline CoNiFe thin films prepared by cyclic voltammetry [J]. *Materials Science Forum*, 2009, 620–622: 731–734.
- [13] LI Jian-feng, ZHANG Zhao, YIN Jun-ying, YU Geng-hua, CAI Cao, ZHANG Jian-qing. Electrodeposition of crystalline CoNiFe soft magnetic thin film [J]. *Transactions of Nonferrous Metals Society of China*, 2006, 16(3): 659–665.
- [14] OSAKA T. Electrodeposition of highly functional thin films for magnetic recording devices of the next century [J]. *Electrochim Acta*, 2000, 45: 3311–3321.
- [15] XIA F F, WU M H, WANG F, JIA Z Y, WANG A L. Nanocomposite Ni–TiN coatings prepared by ultrasonic electrodeposition [J]. *Current Applied Physics*, 2009, 9: 44–47.
- [16] LIU J G, YAN C W. Electrochemical characteristics of corrosion behavior of organic/Dacromet composite systems pretreated with gamma-aminopropyltriethoxysilane [J]. *Surface & Coatings Technology*, 2006, 200: 4976–4986.
- [17] EL-MAHDY G A, NISHIKATA A, TSURU T. AC impedance study on corrosion of 55%Al–Zn alloy coated steel under thin electrolyte [J]. *Corrosion Science*, 2000, 42: 1509–1521.

# 含硼、磷添加剂对电沉积 CoNiFe 软磁薄膜的影响

李建梅<sup>1</sup>, 张 昭<sup>2</sup>, 李劲风<sup>3</sup>, 薛敏钊<sup>1</sup>, 刘燕刚<sup>1</sup>

1. 上海交通大学 化学化工学院, 上海 200240;

2. 浙江大学 化学系, 杭州 310027; 3. 中南大学 材料科学与工程学院, 长沙 410083

**摘 要:** 采用循环伏安法制备 CoNiFe、CoNiFeB 和 CoNiFeP 软磁薄膜。采用 SEM、EDS 和 XRD 进行薄膜形貌、成分及相组成分析, 应用振动样品磁强计(VSM)测量其软磁性能, 并采用电化学阻抗谱(EIS)及极化曲线研究其腐蚀阻力。结果表明, 电沉积 CoNiFe、CoNiFeB 和 CoNiFeP 软磁薄膜为晶态和非晶态混合体, 含硼、磷添加剂可促进非晶相的形成; CoNiFe 和 CoNiFeB 具有纳米结构; 含硼添加剂可提高薄膜的致密度和阻力, 并使矫顽力从 851.48 A/m 降低至 604.79 A/m, 而磁饱和强度基本不变。含磷添加剂可增加薄膜粒子的尺寸并降低其耐蚀性, 并使 CoNiFeP 薄膜的矫顽力增加至 12485.79 A/m, 磁饱和强度大幅度降低至 1.25 T。

**关键词:** 磁性材料; 薄膜; 电沉积; 磁性能; 腐蚀

(Edited by Xiang-qun LI)